Spectral Analysis of the SOHO/LASCO Satellite CME counts, Sunspot Numbers, and Dst Index: Implication to Space Weather Predictions

Nicholas San Juan, David Chappell, Esayas Shume

University of La Verne, La Verne, CA

Introduction

This poster presents correlation analysis of frequency of occurrences of Coronal Mass Ejections (CMEs) and a measure of geomagnetic storms, namely, the Disturbance storm-time (Dst) Index. A multi-scale cross-spectral analysis technique has been employed to investigate the relationship between frequency of occurrences of CMEs and the strength of Dst Index. A quantitative measure of this relationship is estimated using coherence and phase (lead/lag) of the cross spectra between frequency occurrences of CMEs and the strength of the Dst Index with a measure of statistical significance. The coherence and phase of the two time series provide information that could be used to develop a system which can be utilized to forecast space weather.

Database

Fig. 1 displays long-term observations of the sunspot numbers, the frequency of occurrences of CMEs (NASA SOHO LASCO), and the Dst index. The top panel shows a large negative excursion of the Dst index for an increase in CME occurrence indicating a cause-effect relationship. Along with the bottom panel, the co-variation of the three signals agrees well with the well-known 11-year sunspot cycle periodicity. We will be using a section of this data for multi-scale spectral analysis in this poster.

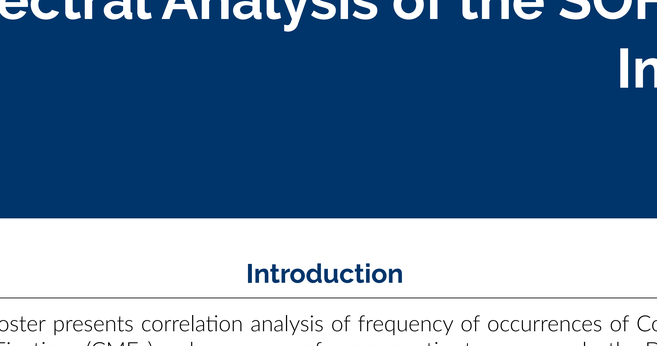

Figure 1. Time series of Dst index, frequency of occurrence of CMEs, and Sunspot Numbers.

Noise Characterization

The purpose of estimating the background noise is to provide a measure of statistical significance of our spectral power calculations. We model the background noise y_n of each signal as red noise described by

$$y_n = A\left[\alpha_{AR1}\, y_{n-1} + z_n\right]$$

where α_{AR1} is the lag-1 autocorrelation coefficient, A is the noise amplitude and z_n is a stochastic variable drawn from a normalized Gaussian distribution. We fit the theoretical red noise power spectrum given by

$$P_k = \frac{A^2\left(1-\alpha_{AR1}^2\right)}{1+\alpha_{AR1}^2-\alpha_{AR1}\cos(2\pi k/N)}$$

to the power spectrum of each signal, excluding frequencies with clear enhanced power.

Fig. 2 shows the power spectrum and best fit red noise spectra for the daily sunspot counts, Dst index and the daily CME counts. The dashed red line shows the 3σ (99.7%) significance level [2].

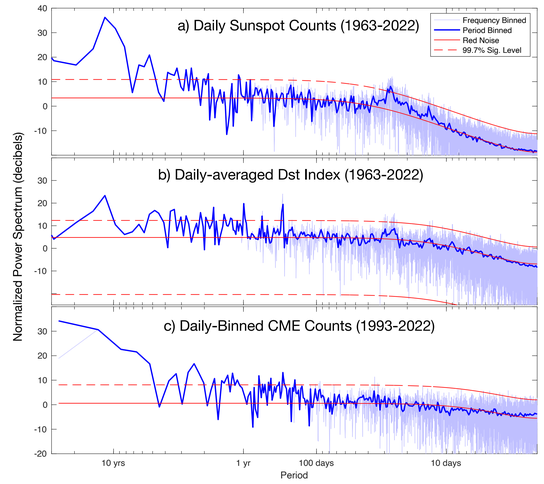

Figure 2. Power spectra of (a) daily sunspot counts, (b) the Dst index and (c) the daily number of CME events. The solid red curve shows the fitted red noise spectrum with fitted parameters (a) $\alpha_{AR1} = 0.85$ and $A = 0.412$, (b) $\alpha_{AR1} = 0.59$ and $A = 0.887$ and (a) $\alpha_{AR1} = 0.34$ and $A = 0.753$.

Continuous Wavelet Transform

The Continuous Wavelet Transform (CWT) is a multi-scale spectral analysis technique employed in our investigation. Mathematically, this technique can be described as

$$X_w(s,k) = \frac{1}{\sqrt{s}}\int_{-\infty}^{\infty} x(t)\Psi\left(\frac{t-k}{s}\right)dt \tag{1}$$

The parameter s in equation 1 is a scaling parameter whose use is to stretch and compress the wavelet function Eqn. 2 to find variations within the signal. The parameter k is a translation parameter whose use is to propagate the wavelet function across a signal.

The Morlet wavelet function Eqn. 2 is employed in the analysis of this work [2].

$$\Psi = k_0 e^{i\omega t} e^{-t^2/2} \tag{2}$$

When we apply the wavelet analysis technique on the Sunspot signal (Fig. 3), the well-known 11 year periodicity is reproduced.

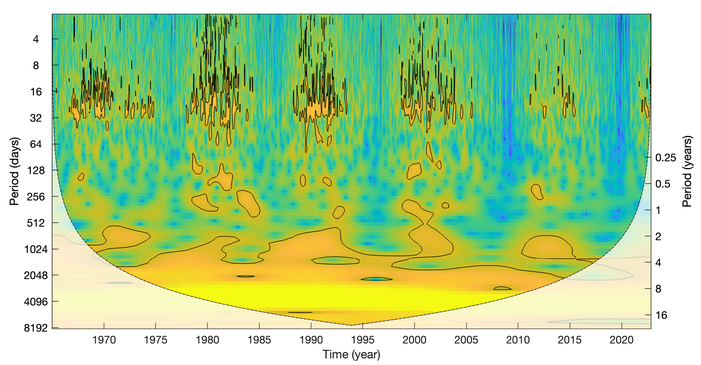

Figure 3. Wavelet Transform of Sunspot numbers

Cross-Wavelet Transform

The Wavelet Coherence can be used to identify both frequency and time intervals when time series were related but do not necessarily have high power.

$$R(s,k) = \frac{2|X^{XY}(s,k)|^2}{|X^X(s,k)|^4 + |X^Y(s,k)|^4} \tag{3}$$

The Coherence plot give us information about the phase and lag between two time series given by:

$$\phi_n = \tan^{-1}\left(\frac{\Im(X^{XY})}{\Re X^{(XY)}}\right)$$

where $-\pi \geq \phi_n \leq \pi$. $\phi_n > 0$, X leads Y [1, 3].

Fig. 4 shows a segment (July 2015) of the Dst index and frequency of occurrence of the CME data in Figure 1. The top and bottom panels of Fig. 4 present the coherence and phase of the cross-wavelet power spectra applied on the segment (July 2015) of the Dst index and the CMEs data. In regions of high coherence (close to about 1, top on Fig. 4), the phase difference (bottom panel, Fig. 4) falls within the ranges of about $-\pi/2$ to $\pi/2$ (within a lead/lag time of about a week). These are coarse estimates of lead/lag relationship of the Dst index and frequency of occurrence of the CMEs.

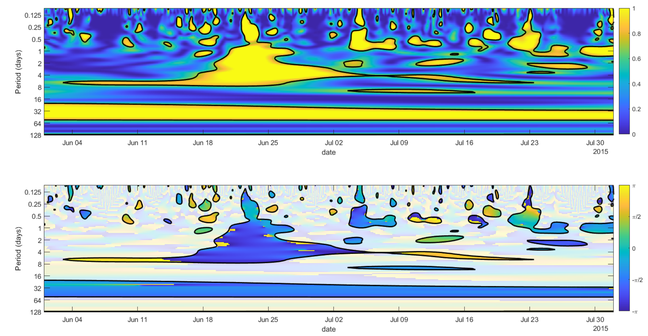

Figure 4. Coherence and Phase plots of Dst index and CME data

Conclusion

We have conducted a preliminary analysis of the relationship between the occurrence of frequency of CMEs and the Dst index using phase and coherence of multi-scale power spectra of the two parameters. In regions of high coherence, the phase difference between the occurrence of frequency of coronal mass ejections and disturbance storm time index falls within a lead/lag time of about by a week. Following this preliminary study, further extensive data analysis will be performed to develop a system which can be useful for space weather forecasting.

References

[1] Aslak Grinsted, John C Moore, and Svetlana Jevrejeva. Application of the cross wavelet transform and wavelet coherence to geophysical time series. *Nonlinear processes in geophysics*, 11(5/6):561–566, 2004.

[2] Christopher Torrence and Gilbert P Compo. A practical guide to wavelet analysis. *Bulletin of the American Meteorological society*, 79(1):61–78, 1998.

[3] Christopher Torrence and Peter J. Webster. Interdecadal changes in the enso–monsoon system. *Journal of Climate*, 12(8):2679 – 2690, 1999.